GSICS Global Space-based Inter-Calibration System

Quarterly

Newsletter – Fall 2014 Issue

Volume 8 Number 3
2014
doi: 10.7289/V5K0726J

Manik Bali, Editor

This Issue:

Special Issue on Visible Calibration

In This Issue

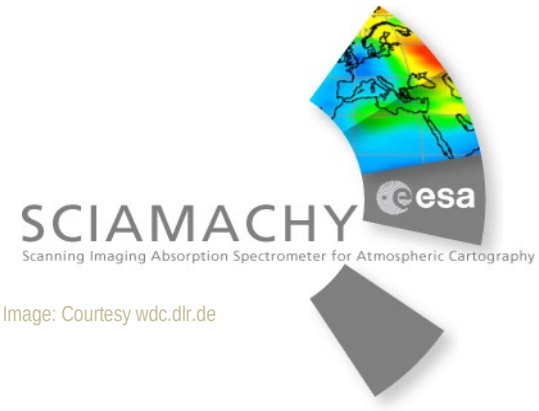

Image: Courtesy wdc.dlr.de

Himawari-8 launched on 7 October 2014 from the Tanegashima Space Center in Kagoshima, Japan.

SBAF web tool based on SCIAMACHY Hyper-Spectral Radiances

by David Doelling and Benjamin Scarino, NASA

The current GSICS visible reference calibration is based on Aqua-MODIS channel 1 (0.65 µm), and in the future will be established from overlapping sequential MODIS/VIIRS visible imager data, traceable to an eventual well-calibrated hyper-spectral imager (e.g., CLARREO). Regardless of whether the Aqua-MODIS reference radiances are used directly to calibrate a target satellite imager by ray-matching or simultaneous nadir overpass comparisons, or are used to characterize invariant lunar or Earth targets, a spectral band adjustment factor (SBAF) must be applied to account for spectral response discrepancies between the reference and target sensor. Historically, pseudo-invariant desert targets were spectrally pre-characterized by aircraft, ground, or satellite measurements. A radiative transfer model predicted the target sensor radiance, cold bright targets were assumed to be spectrally flat for wavelengths less than 1 µm. At present, several GPRC's use coincident MODIS cloud properties to predict the target radiance.

Alternatively, Doelling et al. (2012) tested whether hyper-spectral footprint radiance measurements convolved with target and reference spectral response functions (SRFs) could predict the SBAF over an invariant target or a ray-matching domain. The study demonstrated the inter-calibration of GOES-12 and Aqua-MODIS using ray-matched radiance pairs over land and water, separately. SCIAMACHY hyper-spectral SRF-convolved radiances, i.e., pseudo target and reference radiances, were linearly regressed in order to derive two distinct SBAF values specific to land and water. The resulting land and ocean GOES-12 gain difference, with consideration of the SBAFs, was less than 0.3%, whereas the

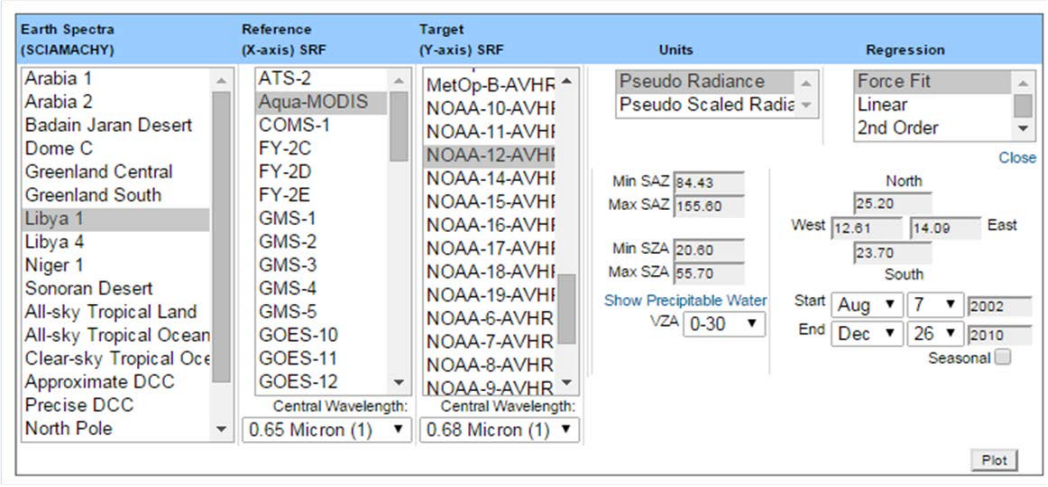

Figure 1. Screen capture of SBAF selection web tool Version 1

difference was 4.7% without application of the SBAFs. Doelling et al. (2013) found that the Aqua-MODIS and SCIAMACHY relative radiances were stable to within 0.6% per decade. This level of stability supports that the ~10-year SCIAMACHY record is suitable for deriving SBAFs. The study concluded that independent Meteosat-9 calibration gains, based on DCC, Libya-4 pseudo-invariant desert, Aqua-MODIS ray-matching, and SCIAMACHY ray-matching techniques, were within 1% of each other owing to the fact that scene-specific SCIAMACHY-based SBAFs were applied for each method, and because all gains were referenced to Aqua-MODIS.

Envisat (10:00 AM sun-synchronous orbit) SCIAMACHY Level-1b, Version-7.03 hyper-spectral measurements, from August 2002 through December 2010, were collected into a database. A total of 3200 SCIAMACHY hyper-spectral radiances are associated with each nadir-scan-mode, 30 x 240-km footprint. Supporting data, e.g,, footprint-centered viewing geometry, latitude, longitude, time, and collocated GEOS-4 precipitable (PW) content, were also saved. The global database was subsetted into GEO/LEO inter-calibration domains (All-sky tropical land and ocean) and LEO/LEO domains (North and South pole). Clear-sky desert sites, all-sky Dome-C and Greenland sites, tropical clear-sky ocean, and DCC footprints, were identified as well. These Earth spectra can be further subsetted by angle, location, time and PW; however, PW is not available for all footprints. Users choose the reference and target spectral bands, the unit preference of either pseudo radiances or reflectances (scaled radiances), and finally the regression type (Fig. 1). More detailed information regarding the SBAF web tool can be found in Scarino et al. (2014). The tool can be accessed at http://angler.larc.nasa.gov/SBAF/.

To illustrate the subsetting capabilities of the SBAF selection tool, Aqua-MODIS and NOAA-12-AVHRR 0.86-µm SCIAMACHY-based pseudo scaled radiances measured from Libya-1 were linearly regressed through the origin. Respectively, Figs. 2a and 2b indicate an SBAF of 0.884 when measurements are limited to those footprints with a PW value less than 0.75 g cm^{-3}, and slope of 0.839 for those with a PW value greater than 2.0 g cm^{-3}. The significant change of adjustment factors is due to the narrower Aqua-MODIS channel-2 SRF being situated between strong water vapor absorption bands that are encompassed by the corresponding AVHRR channel-2 SRF. That is, the increased absorption owed to PW has reduced the AVHRR radiance compared to MODIS, and therefore decreased the SBAF. The SRFs can be compared at the following web site: http://angler.larc.nasa.gov/SPECTRAL-RESPONSE.

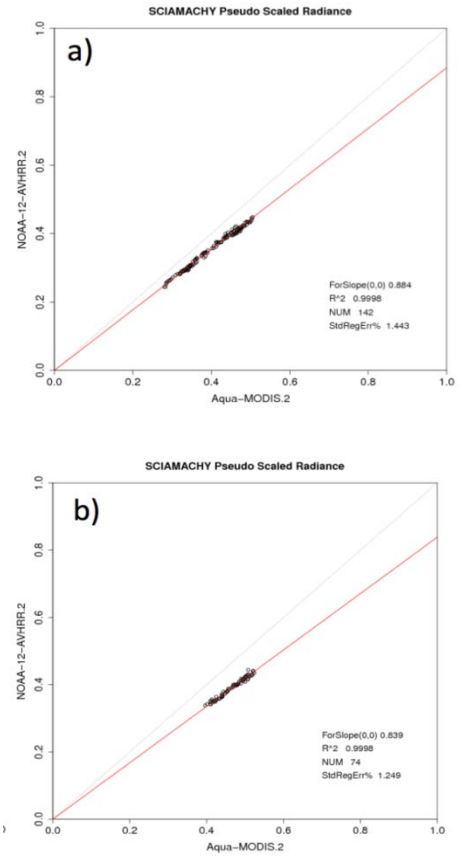

Figure 2.SBAF selection tool output for Libya -1 for PW intervals of (a) 0.0-0.75 g cm^{-3} and (b) 2.0-3.0 g cm^{-3}

Return to Page 1

The accuracy of the SCIAMACHY-based SBAF was compared with GOME-2 and Hyperion during August 2007 over the Libya-4 pseudo-invariant desert site (Scarino et al. 2014). The mean spectra from 17 SCIAMACHY footprints, 17 GOME-2 footprints, and 5 Hyperion overpass swaths were used to compute the Aqua-MODIS-divided-by-NOAA-14-AVHRR pseudo radiance ratio for both the 0.65-µm and 0.86-µm channels. The SCIAMACHY, GOME-2, and Hyperion ratios were 0.9811, 0.9783 and 0.9789, respectively for the 0.65-µm channel. For the 0.86-µm channel, the ratios were 0.8487 and 0.8474 for SCIAMACHY and Hyperion, respectively.
Because the SCIAMACHY based SBAF is within 0.3% of that from GOME-2 and Hyperion for the 0.65-µm channel, and within 0.1% of that from Hyperion for the 0.86-µm channel, SCIAMACHY is therefore comparable to other contemporary hyper-spectral instruments. Furthermore it is the best suited, of the three sensors, for SBAF computations given that it is globally available, has a high spectral resolution, and has a relatively large spectral range.

References:

Doelling, D. R., C. Lukashin, P. Minnis, B. Scarino, and D. Morstad., 2012, Spectral reflectance corrections for satellite intercalibrations using SCIAMACHY data. *IEEE Geosci. Remote Sens. Lett*., vol. 9, no. 1, pp. 119–123

Doelling, D.R., et al.,2013, The intercalibration of geostationary visible imagers using operational hyper-spectral SCIAMACHY radiances. *IEEE Trans. Geosci. Remote Sens.*, vol. 51, no 3., pp. 1245-1254

Scarino, B., et al., 2014, A Web-based Tool for Calculating Spectral Band Difference Adjustment Factors Derived from SCIAMACHY Hyper-spectral Data, Submitted to *IEEE Trans. Geosci. Remote Sens, 2014*

Discuss the article

Radiometric Calibration plans for Himawari-8/AHI

by Masaya Takahashi and Arata Okuyama, JMA

The next-generation geostationary meteorological satellite of the Japan Meteorological Agency (JMA), Himawari-8, was successfully launched using H-IIA Launch Vehicle No. 25 at 5:16 UTC on 7 October 2014 from the Tanegashima Space Center in Kagoshima, Japan. The satellite separated from the launch vehicle about 28 minutes after lift-off, and settled into geostationary orbit on 16 October. The satellite is expected to start operation in July 2015 after the completion of in-orbit testing and checking of the overall system including related ground facilities.

Himawari-8 is located at approximately 140 degrees east, and will observe the East Asia and Western Pacific regions as a successor to the current MTSAT-2 satellite. Himawari-8 will feature a new imager, Advanced Himawari Imager (AHI), with 16 bands as opposed to the 5 bands of the MTSAT series. Table 1 shows the observation bands. The imager's horizontal resolution will also be double that of the MTSAT series. Full-disk imagery will be obtained every 10 minutes. Rapid scanning at 2.5-minute

Table 1 The Himawari-8 imager bands compared with MTSAT-2

Band	Himawari-8		MTSAT-2	
	Wavelength [µm]	Spatial Resolution	Wavelength [µm]	Spatial Resolution
1	0.47	1 km	-	-
2	0.51	1 km	-	-
3	0.64	0.5 km	0.68	1 km
4	0.86	1 km	-	-
5	1.6	2 km	-	-
6	2.3	2 km	-	-
7	3.9	2 km	3.7	4 km
8	6.2	2 km	6.8	4 km
9	6.9	2 km	-	-
10	7.3	2 km	-	-
11	8.6	2 km	-	-
12	9.6	2 km	-	-
13	10.4	2 km	10.8	4 km
14	11.2	2 km	-	-
15	12.4	2 km	12.0	4 km
16	13.3	2 km	-	-

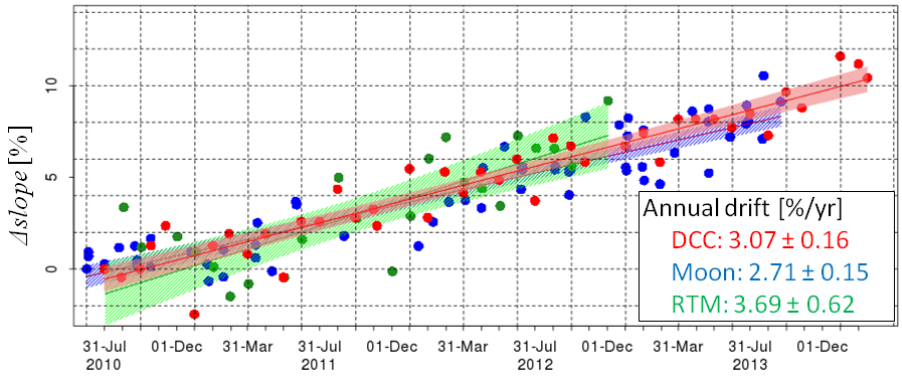

Figure 1: Time series of variation of MTSAT-2 visible calibration slope derived from three calibration methods. Each result is normalized against the first calibration result. Shaded area shows the 95% confidence interval of the linear regression fits.

Return to Page 1

or 30-second intervals will be conducted over several large and small regions. One of the rapid scanning observations will be also be used to derive the moon images for the purpose of visible and near infrared band calibration. These significant improvements will bring unprecedented levels of performance in monitoring for tropical cyclones as well as rapidly developing cumulonimbus and volcanic ash clouds.

As to radiometric calibration of AHI, on-board calibration, inter-calibration and vicarious calibration methods have been developed. AHI has a blackbody and a solar diffuser as on-board calibration system. The former is used for infrared bands in combination with deep space observation. The latter is similar to that for MODIS, designed for visible and near infrared calibration. For infrared bands, inter-calibration based on hyper-spectral infrared sounder (i.e., Metop-A/IASI at present) as a reference sensor will be also performed. JMA has identified three possible visible and near infrared calibration approaches to perform in-orbit calibration of the Himawar-8/AHI. Figure 1 shows comparison of visible channel degradation of MTSAT-2/Imager estimated between three calibration methods: DCC (in red), Moon (in blue), and RTM (in green). These methods have been developed in collaboration with the University of Tokyo and GSICS:

1. "DCC" is an inter-calibration technique that uses deep convective cloud observation as reference calibration targets. This technique has been proposed by NASA GPRC (Doelling et al, 2011). DCC is a statistical approach that compares probability distribution function (PDF) of DCC pixels observed by the geostationary satellite imager with that of the PDF by a reference instrument, Aqua/MODIS. It theoretically provides very stable results because DCCs which reach the tropopause are assumed to have negligible water vapor absorption, and are optically thick behaving as solar diffusers.

2. "Moon" is a calibration method that uses the moon as an invariant calibration target. In this method disc-integrated lunar irradiances are compared between observation and reference to derive the calibration gain. The ROLO (Robotic Lunar Observatory) model developed at U. S. Geological Survey (USGS) provides predicted reference irradiance (Kieffer and Stone, 2005). The moon is also very stable target with no atmosphere. Lunar calibration cannot resolve short term instrument drifts due to infrequent measurements. On the other hand, lunar calibration is suitable for estimating long term instrument degradation due to its small uncertainty.

3. "RTM" is a vicarious calibration using radiative transfer simulation (RTM) (Kosaka and Okuyama, 2012). Simulated radiance of pseudo-invariant clear-sky and spatially uniform cloud targets (i.e., clear-sky ocean, desert, liquid water cloud, and DCC) is compared with that of observations. Coincident and collocated Aqua/MODIS retrievals are used to derive input data for the simulation.

All three methods (DCC, Moon and RTM) provide similar annual drifts (3.07%, 2.71%, 3.69% for DCC, Moon, and RTM, respectively) with small uncertainties for DCC and Moon (±0.16% and ±0.15%). There is clear seasonal cycle in the RTM results, leading to larger calibration uncertainty. This variation is supposedly caused by the assumption of ice crystal shape, optical thickness of DCC pixels and inhomogeneous target selection.

Himawari-8 is expected to be operational in July 2015. Implementation of the above-mentioned calibration methods for Himawari-8/AHI is in preparation. We plan to apply DCC inter-calibration method to the 0.47, 0.51, 0.64, and 0.86 μm bands and also investigate its feasibility with the 1.6 and 2.3 μm bands. Lunar calibration and vicarious calibration using the RTM will be used for all of six visible and near infrared bands. In particular, lunar observations with multiple phase angles derived from rapid scanning at 30-second intervals are expected to be useful to validate the ROLO model stability. Progress will be reported at GSICS annual meeting in March 2015, and calibration monitoring will be also available on the JMA GPRC website: http://ds.data.jma.go.jp/mscweb/data/monitoring/calibration.html

References

Doelling, D., D. Morstad, R. Bhatt, and B. Scarino., 2011, Algorithm Theoretical Basis Document (ATBD) for Deep Convective Cloud (DCC) technique of calibrating GEO sensors with Aqua-MODIS for GSICS. GSICS Wiki [Online], Available: https://gsics.nesdis.noaa.gov/pub/Development/AtbdCentral/GSICS_ATBD_DCC_NASA_2011_09.pdf

Kieffer, H. H., and T. C. Stone., 2005, The Spectral Irradiance of the Moon. *Astron. J.*, 129, 2887-2901.

Kosaka, Y. and A. Okuyama., 2012, MTSAT-2 visible vicarious calibration approach and its monitoring webpage. *GSICS Quart.* doi:10.7289/V5DR2SD2

Discuss the article

doi: 10.7289/V5K0726J
GSICS Quarterly: Special Issue on Visible Calibration Volume 8, No. 3, 2014

Comparison of Absolute Calibration Accuracy between Deep Convective Cloud and Desert Methods for GOES Imager Visible Channels

by Fangfang Yu and Xiangqian Wu, NOAA

High quality calibrated satellite radiances are fundamental to accurately retrieve geophysical products. Vicarious calibration, which uses not-in-orbit stable sites as calibration reference, plays an important role in providing accurate calibrated radiance/reflectance of satellite instruments. It is used to generate post-launch calibration coefficients to compensate for the sensor in-orbit degradation for the instruments without on-board calibration devices, and also used to validate the radiance/reflectance generated with the on-board calibration techniques. To reduce the risk of erroneous degradation trending or calibration coefficients, multiple vicarious calibration methods are often used to cross-check the results. Deep convective cloud (DCC), due to its stable spectral and radiometric spectra and common availability to the Earth observation satellites, is selected by the GSICS community as a common reference for the instrument inter-calibration of satellite visible channels. This article reports our recent work on the absolute calibration of GOES-12 (GOES-East) and GOES-15 (GOES-West) Imager visible channels using DCC and Sonoran Desert as transfers traceable to Aqua MODIS C6 Band1 calibration standard. The GOES DCC pixels are selected following the GSICS DCC algorithm theory baseline document (ATBD) from the spatial domain of ±20^o from the GEO sub-satellite location (Doelling, 2011a). The Sonoran desert observations [32.05^{o}N-32.35^{o}N, 114.4^{o}W-114.7^{o}W] are routinely sorted into subsets and archived everyday from the GOES Northern Hemisphere scan frame close to 12:15pm for GOES-East and 12:35pm for GOES-West.

Table 1: Aqua-MODIS reference reflectance of DCC and Sonoran Desert for GOES-12 and GOES-15.

Reference Targets	GOES-12	GOES-15
DCC (mode reflectance)	87.39±2.11%	90.01±2.10%
DCC (median reflectance)	88.07±1.96%	90.41±1.94%
Sonoran Desert	30.93±2.03%	31.86±1.97%

Accurate determination of the reference reflectance is critical for the absolute calibration accuracy. The DCC reference reflectance is determined with the Aqua MODIS DCC pixels generated from the Ray-matching method, which identifies the pairs of collocated GOES and MODIS pixels scanned at similar viewing zenith angles within a certain time interval (Doelling et al. 2011b). The GOES-MODIS collocations over the ±10^o from the GEO sub-satellite location are used to reduce the BRDF impact, assuming that the DCC reflectance is uniform over the GEO DCC domain. The collocated MODIS DCC pixels from April 2003 through April 2010 and from December 2011 through December 2013 are used to determine the DCC reference reflectance values for GOES-12 and GOES-15, respectively.

Two types of statistical values are used to represent the DCC reflectance: mode and median reflectance of the DCC pixels (Table 1). Statistical analysis shows that at least two thousand DCC pixels are required for a robust monthly DCC reflectance. The number of monthly collocated DCC pixels over the GOES-12 domain ranges from several thousand to tens of thousands for most months from April 2003 through April 2010. Therefore, the mean values of the monthly mode and median MODIS DCC reflectance are used to determine the DCC reference reflectance for GOES-12. The uncertainties of the DCC reflectance are calculated with one standard deviation of the monthly mode and median MODIS DCC reflectances, respectively. The ratio between the desert and mode DCC derived calibration correction coefficients are 0.9893 (GOES-12) and 1.0095 (GOES-15). The corresponding ratios between desert and median DCC methods are 0.9928 (GOES-12) and 1.0077(GOES-15) (Figure 1). Therefore, the systematic difference of the absolute calibration accuracy between the desert and DCC methods is generally less than 1%, except for the GOES-12 mode DCC method. Both of the DCC methods

Return to Page 1

result in correction coefficients larger than the desert one for GOES-12, yet smaller than the values for GOES-15. Considering that GOES Imager scan mirrors may have about 1-2% difference in incidence angle dependent reflectivity (Yu et al. 2013), the biases between these two methods, if corrected with the angle dependent reflectivity for the Sonoran desert data, may be reduced. This is because GOES-12 and GOES-15 view the Sonoran desert at fixed scan angles of approximately -2.5^o and +1.4^o from the nadir respectively, while the DCC pixels are scattered over the sub-satellite region. Results of this study enhance our confidence in applying DCC and desert methods to validate the GOES-R Advanced Baseline Imager (ABI) on-board radiometric calibration accuracy for the corresponding solar reflective channels.

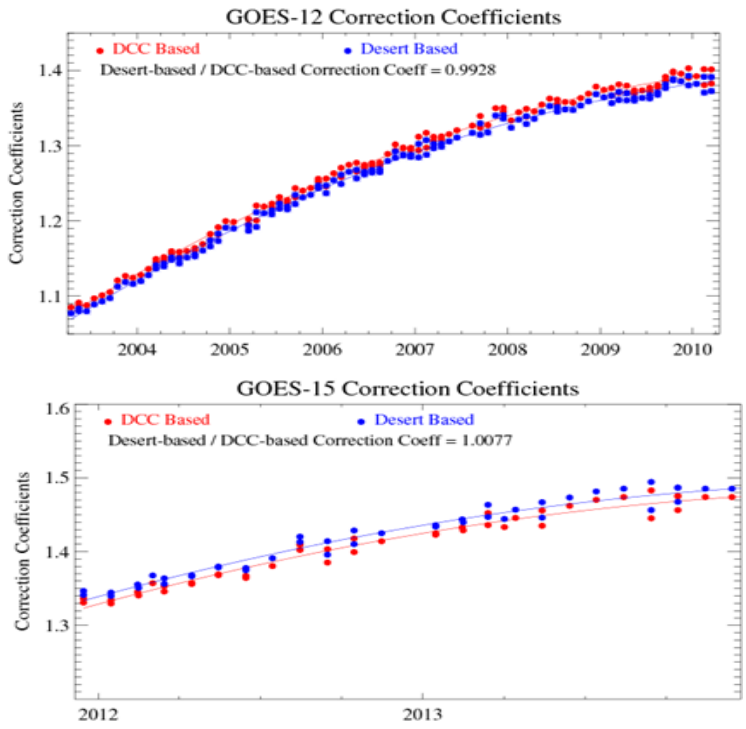

Figure 1: Post-launch correction coefficients derived with DCC (median reflectance) and Sonoran desert methods for GOES-12 (upper) and GOES-15 (lower).

References

Doelling, D., D. Morstad, R. Bhatt, and B. Scarino, 2011a, *ATBD for DCC technique of calibrating* GEO sensors with Aqua-MODIS for GSICS, https://gsics.nesdis.noaa.gov/wiki/Development/AtbdCentral.

Doelling, D., R. Bhatt, D. Morstad, and B. Scarino., 2011b, *ATBD for ray-matching technique of calibrating* GEO sensor with Aqua-MODIS for GSICS, https://gsics.nesdis.noaa.gov/wiki/Development/AtbdCentral.

Yu, F., et al., 2014, Intercalibration of GOES Imager visible channels over the Sonoran Desert, *JGR*, 119, doi:10.1002/2013JD020702.

Yu, F. and X. Wu., 2014, An integrated method to improve the GOES Imager visible radiometric calibration accuracy, *Remote Sensing of Environment* (under review)

Yu, F., et al., 2013. Angular variation of GOES Imager scan mirror visible reflectivity, *GSICS Quarterly Newsletter*,doi:10.7289/V5N877QQ

Discuss the article

Monitoring the Meteosat-9 visible channels using the GSICS Deep Convective Cloud method

by Sébastien Wagner and Tim Hewison , EUMETSAT

Within the framework of the Global Space-based Inter-Calibration System (GSICS) activities, EUMETSAT is implementing a methodology developed by NASA (Doelling *et al. 2011*) based on the use of Deep Convective Clouds (DCC) to transfer the calibration of reflective solar bands from Aqua MODIS to a target instrument aboard a geostationary satellite. This method is currently applied to the VIS06 (0.65µm) band available on the SEVIRI instrument aboard Meteosat-9. The purpose of such work is:

1. to increase EUMETSAT's capabilities to monitor the visible channels on the current operational geostationary missions (Meteosat-7, -8, -9 and -10);
2. to provide GSICS Near-Real Time and Re-Analysis Corrections (NRTC and RAC, respectively) to users in order to improve the retrieval of geophysical parameters using better calibrated Level 1 data.

The EUMETSAT implementation of the algorithm comprises two major steps to allow a faster partial reprocessing, re-analysis and sensitivity analysis:

a) The detection and extraction of the DCC pixels to create intermediate data sets.

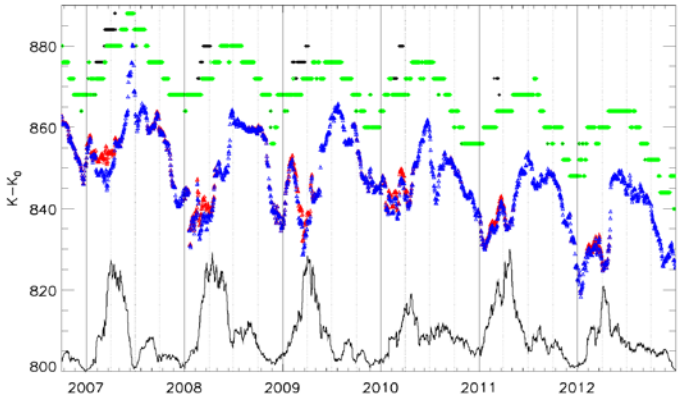

Figure 1: Time series of mode (top) and mean (middle) and number (bottom) of extracted reference DCC counts for Meteosat-9 VIS06 band between 01/10/2006 and 31/12/2012, above oceans (in blue) and above land (in green) and both (in red). The plain black line represents, for illustration, the evolution in time of the number of DCC pixels.

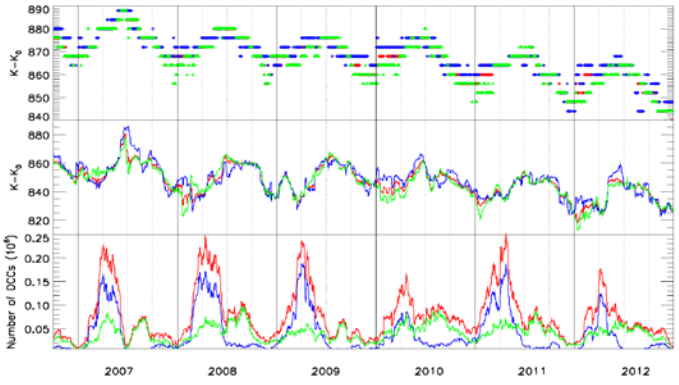

Figure 2: Time series of the extracted reference DCC counts for the Meteosat-9 VIS06 band between 01/10/2006 and 31/12/2012. In black: mode with saturated signal. In green: mode without saturation. In red: the mean with saturation. In blue: the mean without saturated signal. The plain black line represents, for illustration, the evolution in time of the number of DCC pixels

b) The derivation of GSICS corrections with additional filtering (in particular on the homogeneity of the cloud fields) and the application of the Bi-directional Reflectance Distribution Function (BRDF) to normalize effects due to viewing geometry for both the Aqua MODIS and the target instrument datasets. A spectral band adjustment factor (SBAF) is applied to the Aqua-MODIS pixel radiances to account for the spectral differences between the two instruments. Similarly to the GSICS infrared products, these corrections are derived over a sliding window of 31 days backward in time for NRTC and centered in time for RAC.

In order to test and validate this implementation of the GSICS DCC method the complete archive of full disk images acquired by Meteosat-9 was processed. It extends from October 2006 to December 2012. As from January 2013, images acquired with the Scan Service were not processed as the geographical coverage is outside the range of applicability of the method. The analysis revealed two issues:

- Meteosat-9 VIS06 band saturated regularly over DCCs
- A seasonal cycle is observed in the digital count, which is proportional to radiance, time series derived from the derived Probability Density Functions (mean and mode).

Figure 1 illustrates how the count time series change in time when dealing or not with the saturated signal, and when using the mode or the mean derived from the associated Probability Density Functions. Whereas saturation has a relatively strong impact in the early time of the mission (black and red curves), its effects are decreasing in time due to the natural degradation of the instrument. In order to prevent saturation from biasing the monitoring results, it is removed from the data through a simple check on the maximum count value reached by the instrument above the identified DCCs.

Figure 1 also shows the seasonality observed in the time series. Data were filtered according to the type of scenes (land/ocean) in order to check if the seasonality is caused by the occurrence of convection above land or oceans at specific times of the year. Figure 2 summarizes the results of these tests. The seasonality clearly remains in all three time series. However, the bottom panel of Figure 2 shows the strong seasonal variability between ocean and land in terms of DCC sampling. Additional tests are on-going to look at the geographical location of the DCC pixels and a possible spatial correlation with the seasonality observed in the data. Currently, the seasonality is removed by a mathematical analysis of the accumulated data. Seasonal factors are estimated on a yearly basis using the complete data set. These factors are applied to the original time series using the following multiplicative model:

$$\boldsymbol{Y_{Obs} = Y_{Trend} \cdot Y_{Seasonality} \cdot Y_{Variab}}$$

Where $\boldsymbol{Y_{Obs}}$ is the observation, $\boldsymbol{Y_{Trend}}$ is the overall trend of the time series, $\boldsymbol{Y_{Seasonality}}$ is the seasonal signal and $\boldsymbol{Y_{Variab}}$ is the remaining variability.

Figure 3 illustrates the impact of applying the seasonal corrections to the mode and mean time series. The most significant impact is observed for the mode (dark green), whereas large variations remain in the time series for the mean (dark blue). A linear regression provided the drift estimates from the deseasonalised datasets. The drift is about 0.433% per year using the mode, and 0.417% per year using the mean. Uncertainties on these estimates are respectively 0.003% and 0.006%.

Return to Page 1

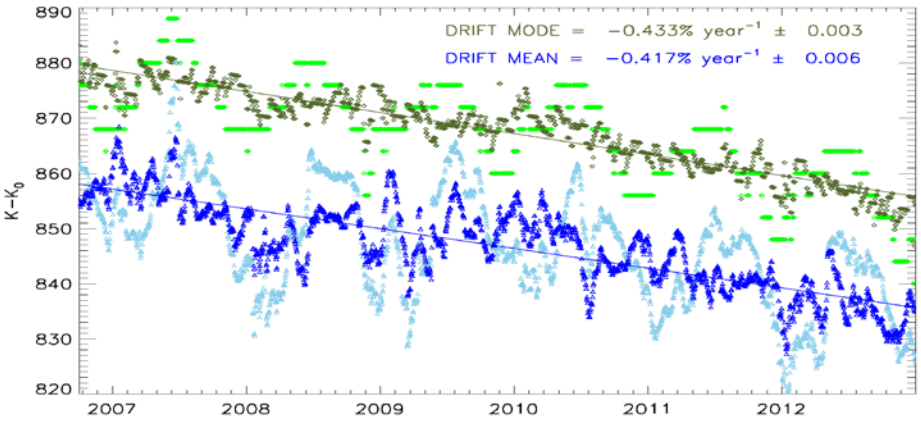

Figure 3: Time series of extracted reference DCC counts (land and oceans) for Meteosat-9 VIS06 band between 01/10/2006 and 31/12/2012. Light green and light blue: original mode and mean DCC counts. Dark green and dark blue: de-seasonalised mode and mean DCC counts.

The GSICS DCC method has been successfully applied to the Meteosat-9 VIS06 band. In order to infer more robust drift estimate, the saturated counts were removed and the data was de-seasonalized. Accounting for the uncertainties, the resulting DCC trend is consistent with the drift estimates derived using lunar observations (Viticchiè et al., 2013a, Viticchiè et al., 2013b) (0.499% per year with 0.018% uncertainty) and using the uncertainty) and the SEVIRI Solar Channel vicarious Calibration system (Govaerts *et al., 2004*) (0.293% per year with 0.156% uncertainty). Future work will include the extension of the method to the VIS08 band. In order to address imagers with shorter time series, a better understanding of the seasonality is essential to infer robust drift estimates. Ultimately, a GSICS correction will be derived using the MODIS instrument aboard the Aqua satellite as a reference.

References

Doelling D., D. Morstad, R. Bhatt, B. Scarino, 2011,*GSICS ATBD for Deep Convective Cloud technique of calibrating GEO sensors with Aqua-MODIS* https://gsics.nesdis.noaa.gov/wiki/Development/AtbdCentral

Govaerts, Y. M., Clerici, M., and Clerbaux, N., 2004, Operational Calibration of the Meteosat Radiometer VIS Band. *IEEE Transactions on Geoscience and Remote Sensing*, 42, 1900

Viticchiè B., Lunar Calibration of MSG/SEVIRI Solar Channels. 2013, *EUMETSAT conference proceedings*, 2013, Vienna

Viticchiè B. 2013, Lunar Calibration of MSG/SEVIRI Solar Channels GSICS *GSICS Quarterly Newsletter*, doi:10.7289/V5N877QQ

Discuss the article

Dunhuang Site Vicarious Calibration of the VISSR/FY-2 Imager

by Yuan Li, Zhiguo Rong and Feng Lu, CMA

The main payload of China's first-generation geostationary meteorological satellites Fengyun-2 (FY-2) -- the Visible Infrared Spin Scan Radiometer (**VISSR**, Figure 1) -- includes one visible and four infrared channels **(**Jianmin2010; Jianmin et al. 2010). The onboard calibration instruments of **VISSR** contain a half light path blackbody and a sun image monitor. **VISSR** and its calibration instruments had experienced rigorous laboratory and field vicarious calibration before launch (Figure 2; Ni-Na et al. 2007). The sun image monitoring (Figure 3; Fu-Chun and Gui-Lin 2007) and site vicarious calibration (Yuan et al. 2009) of the visible channels have been performed every year since launch.

From 11 August to 29 August 2013, more than 30 persons from 7 Bureaus have conducted a joint radiometric

Figure 1: Visible Infrared Spin Scan Radiometer

Figure 2: Field vicarious calibration before launch

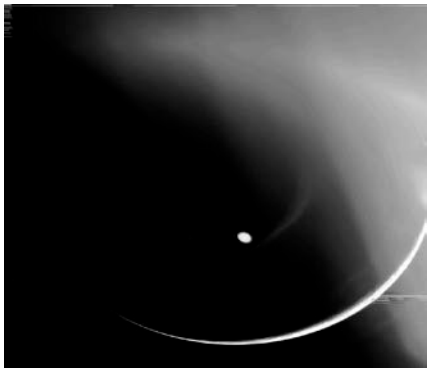

Figure 3: Sun image and stray lights in the visible channel.

calibration experiment (CRCS [China Radiometric Calibration Site] 2013) at the Dunhuang, China site. Surface reflectance was measured by an ASD

Figure 4 Sample position in DH site (Blue point: vertical reflectance; Red point: vertical reflectance and BRDF)

spectrometer and the reference panel which was made by AIOFM. Aerosol Optical Depth (AOD) and Ozone content were measured by CE318 and Microtops II photometers. Water content was measured by the GTS1 digital radiosonde. The 6S model for radiative transfer was used to simulate the apparent reflectance. For VISSR, the output voltage rather than DC is linearly related to the input radiant energy. A lookup AD relation table is needed during calibration.

Dunhuang Gobi surface BRDF

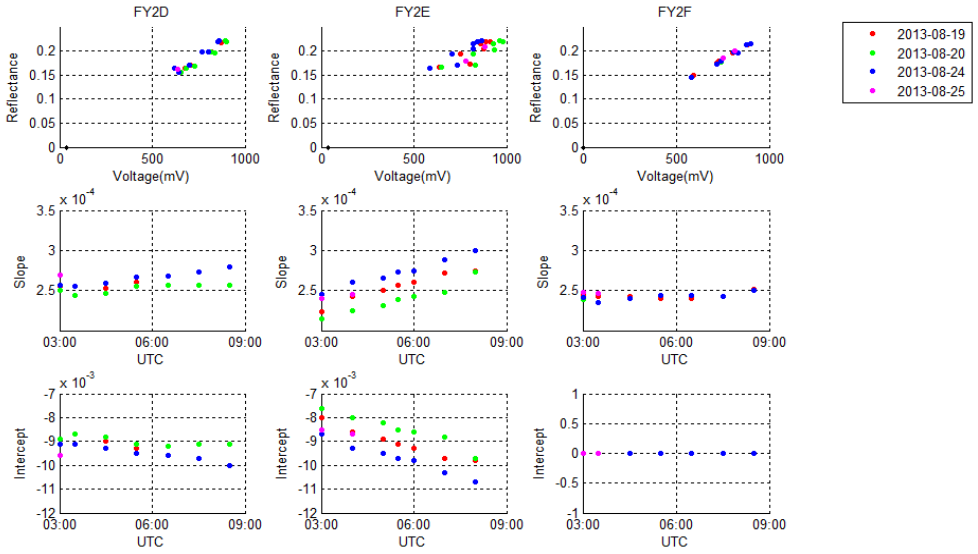

Figure 5:. Calculation of the calibration coefficients via linear regression forced through the origin.

measurements were made during the CRCS 2013 experiment. In order to match the spatial resolution (1.25km) of FY-2, 3x3 sample points were selected covering the 10x10km area (Figure 4). The Ross-Li BRDF model was used to derive the BRDF coefficients.

Since the directional reflectance character of the surface relied on the seasonal reason, BRDF model only represents the character during the measurement time. At other times, the vertical reflectance was measured at eleven sample positions (Blue and Red points in Figure 4) to correct the BRDF model coefficients.

The output voltage had been subtracted from the voltage when the VISSR viewed cold space, so when the output voltage is zero, the corresponding input reflectance should be zero. Consequently, the calibration coefficients were calculated using the linear regression method which was forced to pass through the zero point of voltage and reflectance. The stray lights of FY-2s have not been removed in the operational data.

The changing of stray lights at spatial and temporal region is critical issue especially for FY-2E. This phenomenon makes the calibration uncertainty greater than for the other two satellites.

Return to Page 1

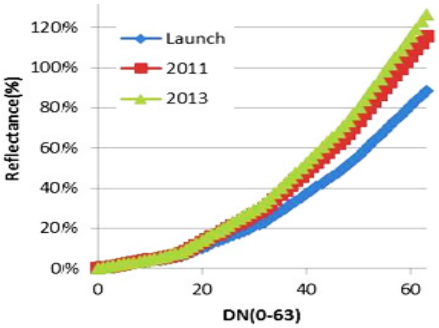

Figure 6: Calibration lookup table (FY-2D).

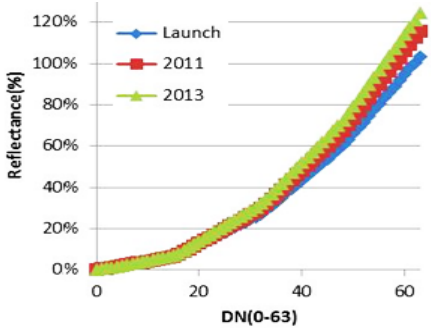

Figure 7: Calibration lookup table (FY-2E).

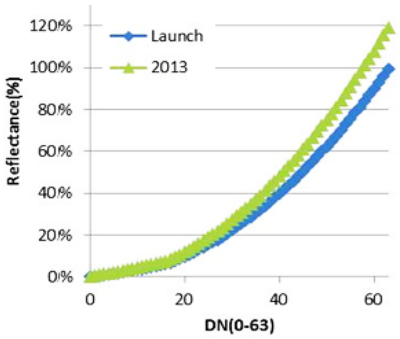

Figure 8: Calibration lookup table (FY-2F).

By comparing the calibration coefficient before launch and August 2013 site calibration, a response decay was found: at 50% reflectance, FY-2D, FY-2E and FY-2F decayed 17.66%, 9.13% and 9.22% respectively (See Figure 6, Figure 7 and Figure 8).

Validation by the DCC method shows that the uncertainty was below 5%. The broadcasting calibration Look-up table is to be updated soon.

References

Jianmin, X, 2010, Development and Trend of China Meteorological Satellite. *Science & Technology Review*, 28(6), 3. (in Chinese)

Jianmin, X, Jun, Y., Zhiqing, Z, et al., 2010, Chinese meteorological satellites, achievements and applications. *Meteorological Monthly*, 36(7), 94-100. (in Chinese)

Ni-Na, P., Jun, L., Wei-Ning, Y, et al., 2007, Comparisons and analyses of pre-launch field radiometric calibration methods for the visible channel of scanning radiometer. *Infrared and Laser Engineering*, 36(5), 597-601(in Chinese)

Fu-Chun, C., and Gui-Lin, C., Comparison between pre-launch and in-orbit visible onboard calibrations . *Chinese Journal of Quantum Electronics*, 24(6), 709-713 (in Chinese)

Yuan, L., Zhang, Y., Jingjing, L., et al., 2009, Calibration of the visible and near-infrared channels of the FY-2C/FY-2D geo meteorological satellite at radiometric site. *Acta Optica Sinica*, 29(1), 41-46 (in Chinese)

Discuss the article

Assessment of the FY2D/E visible imager operational calibration based on DCC

by Lin Chen, CMA

The Fengyun (FY)-2 series satellites are the first generation geosynchronous (GEO) Earth observation satellites operated by the National Satellite Meteorological Center (NSMC). The main payload on FY2 is the multi-spectral scanning radiometer, which is developed by Shanghai Institute of Technical Physics, Chinese Academy of Science. The first generation of China's geostationary meteorological satellites can be divided into three batches. Batch 1 includes two satellites, FY-2A and FY-2B, which were test satellites for the FY-2 series and no longer operating on obit. FY-2C, FY-2D, and FY-2E are included in batch 2. There are Stretched Visible Infrared Spin Scanning Radiometer (SVISSR) on-board FY-2 batch 2 satellites providing hourly images nominally and half-hourly images during flood season. Currently, except FY2C, Batch 2 satellites (FY2D and FY2E) are still operationally running on-orbit. FY2D and FY2E located at 86.5° E and 105° E, respectively

Accurate calibration is the basis and foundation for applications of meteorological information. The visible channel calibration coefficient tables for FY2D and FY2E were obtained during a pre-launch field experiment and were never evaluated while in orbit. Here, deep convective clouds (DCCs) are used as invariant calibration target to verify the stability of FY2D and FY2E visible imagers. The Terra/MODIS DCC reflectance is used as the radiometric reference. The main method followed the Algorithm Theoretical Basis Document (ATBD).

Table 1: Detailed parameters used in the DCC method

	FY2/VISSR	Terra/MODIS
Channels used	Visible channel 10.3-11.3 atmospheric window channel	Channel 1 Channel 31
Data version	Collection 1 published by NSMC	Collection 5 published by NASA
Data time period	Feb., 2007 to Dec., 2013 for FY2D Dec., 2009 to Dec., 2013 for FY2E	Feb., 2007 to May, 2010
Latitude Geographical extent	15°N to 15°S ocean only	15°N to 15°S ocean only
Longitude Geographical extent	65°E to 105°E for FY2D 85°E to 125°E for FY2E	30°E to 140°E
Solar Zenith Angle	< 40°	< 40°
View Zenith Angle	< 40°	< 40°
DCC threshold	< 205K and the BT11μm has been corrected by inter-calibration method	< 205 K
Brightness Temperature Homogeneity	Standard deviation BT 11μm< 1°K	Standard deviation BT 11μm< 1°K
Visible Radiance Homogeneity	Standard deviation R 0.6μm<3%	Standard deviation R 0.6μm<3%
Time range at GEO sub-sat longitude	00 to10 UTC	Not considered
DCC BRDF model	CERES ice cloud(τ>50) ADMs	CERES ice cloud(τ > 50) ADMs
DCC reflectance calculation	Mean value for 30 days, moving day by day	30-day mean

Due to the infeasibility of downloading large volumes MODIS through the internet, only Collection 5 Terra/MODIS data are used here, which did not coincide with the FY2 data record. The apparent difference with ATBD is the DCC reflectance calculation. We used a 30-day running mean to obtain daily reflectance values for FY2 and monthly mean reflectance for MODIS. Some literature has shown brightness temperature bias for FY2 infrared channels and that this bias could be corrected by inter-calibration method using AIRS or IASI (Hu et al. 2013). Although DCC is rather

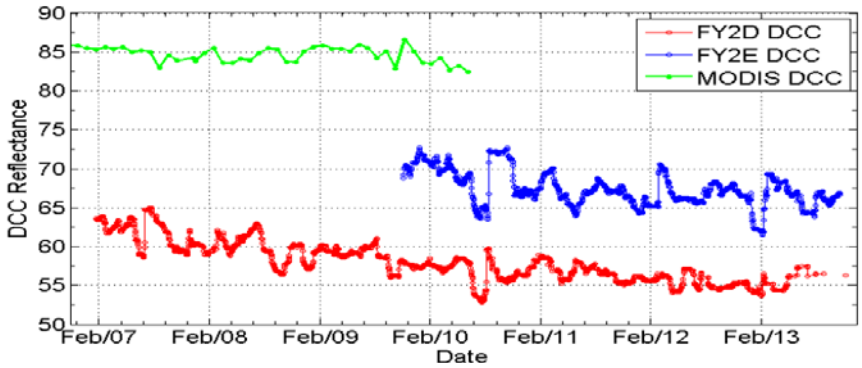

Figure 1. The DCC reflectance of FY2D, FY2E and Terra/MODIS

spectrally flat in the visible spectrum, differences in spectral response functions (SRF) between the reference and reference sensor can introduce a significant error to the inter-calibration. The SRF differences can be accounted for by developing spectral band

Return to Page 1

adjustment factors (SBAF). Here, the simulated hyper-spectral DCC reflectance by SBDART is used. The SBAF for FY2D and FY2E Visible channels to Terra/MODIS channel 1 are 1.009 and 1.008, respectively. In

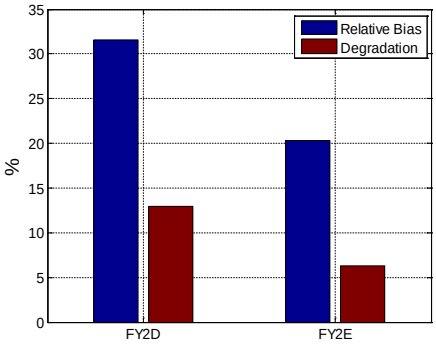

Figure 2: The relative biases between FY2D/E and MODIS DCC and their degradation during their life-times.

order to display and compare the FY2D, FY2E and MODIS DCC in one Figure, the FY2D and FY2E DCC reflectance are divided by the their SBAF respectively.

The Figure 1 shows the DCC reflectance for FY2D, FY2E and TERRA/MODIS.This Figure shows us two apparent facts. One is that there are significant biases between FY2D/E and MODIS. FY2 DCC reflectances is apparent lower than MODIS DCC reflectance. The bias for FY2D is relative bigger than for FY2E. The other fact is FY2D/E visible channels have degraded during their life-time. Figure 2 shows the relative biases between FY2D/E and MODIS DCC and their degradation during their life-times. There was a very large gain increase in 2010 and Feb. 2013 in both FY2D and FY2E. This phenomenon possibly is related to the sun heating on the instrument. The relative biases between FY2D/E and MODIS DCC are 32% and 20%. We use the linear trend to compute the degradation. The relative degradation for FY2D and FY2E are 13.0% and 6.34% during the data time period. We plan to update the FY2 visible channel radiometric calibration table by DCC method in the near future.

References:

Xiuqing Hu, Na Xu, Fuzhong Weng, et al., 2013: Long-Term Monitoring and Correction of FY-2 Infrared Channel Calibration Using AIRS and IASI. *TGRS*, **51(10)**, 5008-5018

D. R. Doelling, D. Morstad, R. Bhatt, and B. Scarino, 2011: Algorithm Theoretical Basis Document (ATBD) for deep convective cloud (DCC) technique of calibrating GEO sensors with Aqua-MODIS for GSICS, https://gsics.nesdis.noaa.gov/pub/Development/AtbdCentral/GSICS_ATBD_DCC_NASA_2011_09.pdf

Discuss the article

News in this Quarter

Committee on Earth Observation Satellites (CEOS)- WGCV 38th meeting held at NOAA, NCWCP

By Changyong Cao and Manik Bali, NOAA

The CEOS/WGCV 38th meeting was held at the NOAA Center for Weather and Climate Prediction (NCWCP) in College Park, MD, USA from September 30 to October 2, 2014, co-hosted by NOAA, NASA, and USGS. More than 40 representatives from 13 countries participated in the meeting. After the welcome speech by Director Dr. Al Powell and his deputy Mike Kalb, the WGCV chair Dr. Satish Srivastava of the Canadian Space Agency delivered the chair report. This was followed by reports from the Terrain Mapping, Infrared Visible Optical Sensors, Microwave, Land product validation, atmospheric composition, and Synthetic Aperture Radar subgroups.

.

Participants of the CEOS WGCV-38 Meeting

The GEO secretariat Osamu Ochiai provided an update from the GEO perspective, in which he praised the WGCV for contributions in the areas of DEM cal/val and QA4EO case studies. The CEOS report was delivered by the Chief Executive Officer Kerry Sawyer, who discussed some of the WGCV roles and responsibilities identified in the CEOS Work Plan, which include cooperation with GSICS, SST and other constellations, and the development of the Radiometric Calibration Network (RADCALNET), in addition to a number of carbon actions as documented in the report of CEOS strategy for carbon observations from space . Progress in the RADCALNET at three instrumented sites (Baotou, China; La Crau, France; and Railroad Valley Playa, US) was reported by the IVOS and respective agencies. Additional sites in Australia and South America were also proposed. Virtual Constellations leads from Atmospheric Composition, Sea Surface Temperature, Precipitation, and Land surface imaging also reported collaboration activities.

GSICS Session

The GSICS session was lead by Mitch Goldberg who highlighted NOAA's JPSS mission and its CAL/VAL activities and shared his experience of participating as the GSICS Executive Panel Chair in CEOS WGCV meetings. Mitch along with Jerome Lafeuille of WMO was instrumental in building the initial bridges between the GSICS and CEOS. Mitch encouraged WGCV to establish surface reference sites and help GSICS with best practices.

Larry Flynn, Director GCC, highlighted the most recent interaction between CEOS and GSICS at WGCV-37 in Frascati and discussed a blueprint for future collaboration. Following an action item on GSICS from CEOS (from WGCV-37), Manik Bali gave a presentation on the GSICS Procedure for Product Acceptance (GPPA). The GPPA is a result of GSICS and CEOS collaboration as the GPPA has been inherited from QA4EO and is used by GSICS to assign maturity to its products. Prof. Jan-Peter Muller from University College London encouraged GPPA to include SNO software standardizations. The collaboration is strengthened by close collaboration between GSICS Microwave (MW) subgroup and WGCV Microwave subgroup. GSICS MW subgroup Chair Dr. Cheng-Zhi Zou, had detailed discussions with WGCV Microwave Sensor Sub-group Chair Xiaolong Dong and they prepared a plan for future cooperation. Similar cooperation will take place with the joint meeting of the CEOS WGCV ACSG and the GRWG UV Subgroup.

With the intent of increasing the collaboration with CEOS, the GSICS Coordination Center invited members of CEOS WGCV to contribute articles to the GSICS Newsletter. As usual, representatives from participating agencies reported cal/val activities by the space agencies around the world. Finally, the meeting participants elected Dr. Kurt Thome of NASA to be the vice chair, together with the new chair Dr. Albrecht von Bargen of DLR for the WGCV. The next WGCV meeting will be held at Berlin, Germany in May 2015.

Discuss the article

Return to Page 1

Annual EUMETSAT Satellite Conference held in Geneva Switzerland

by Manik Bali, NOAA

The 2014 EUMETSAT Meteorological Satellite Conference (#EMSC2014) took place on 22 - 26 September 2014 in the beautiful lakeside city of Geneva, Switzerland. EUMETSAT was joined in the organization and hosting of the event by MeteoSwiss, the national provider for weather and climate services in Switzerland. The conference had nine sessions in all. These included

Session 1 - Current and future satellites, instruments and their applications
Session 2 - Climate
Session 3 - Quantitative applications for nowcasting
Session 4 - Data access for easy utilization
Session 5 - Marine meteorology and oceanography
Session 6 - Instrument calibration and validation campaigns
Session 7 - Atmospheric composition
Session 8 - Satellite data in global and regional modeling
Session 9 - Advances in understanding atmospheric processes using satellite data

The session that was particularly exciting for GSICS members was the Instrument Calibration and Validation Campaigns. Spread over two days (23-24 September 2014), where members had the opportunity to give oral presentation as well as poster presentations . The first part of this session focused on UV and Visible calibration. Berit Ahlers from ESA started the session with her talk on calibrating visible hyperspectral instruments. Talks by Chunhui Pan on OMPS calibration, Fred Wu on GOMES-2 -OMPS comparisons, Dave Doelling on AVHRR calibration and Rajendra Bhatt on transition from Aqua-Modis to NPP-VIIRS gave good overviews of some of the recent advances in UV/VIS calibration. Subsequent parts of this session focused on calibration of Hyper-spectral instruments such as IASI-A/B and CriS.

Fuzhong Weng former Director of GSICS Coordination Center, gave an in-depth analysis of the Suomi NPP satellite instrument CAL/VAL and applications. Likun Wang introduced the CrIS and AIRS and IASI comparisons. Details of the conference program are on the EUMETSAT website.

Presentation on recent advances in using Deep Convective Clouds as calibration targets (Masaya Takahashi) and Lunar calibration (Tim Hewison) were particularly interesting for the calibration community. On the last day of this session, Manik Bali from GSICS Coordination Center (GCC) made a presentation on GSICS products and new initiatives by the GCC. Applications of GSICS products were highlighted in this presentation and members were encouraged to use GSICS products. At the conference Manik Bali and Tim Hewison also prepared and provided copies of a brochure that was distributed to the attendees. This brochure gives a summary of GSICS products and also has examples of uses of the product. Copies of this brochure can be downloaded from the GSICS Coordination Center Website http://www.star.nesdis.noaa.gov/smcd/GCC/documents/GSICSBooklet.pdf. The conference proved to be a magnificent opportunity for attendees to sightsee Geneva as the organizers sponsored a boat ride on Lake Geneva and a dinner at Bâtiment des Forces Motrices (BFM), where GSICS Vice Chair Ken Holmlund gave the welcome speech along with the Swiss organizers. Midway through the conference WMO hosted a side event where key discussions that highlighted the need for international cooperation and cost of climate change were discussed.

The next EUMETSAT Satellite Conference is scheduled to be held in 21 -25 September 2015 in Toulouse, France and members can submit abstracts until the 31st of Jan 2015.

Discuss the article

doi: 10.7289/V5K0726J
GSICS Quarterly: Special Issue on Visible Calibration Volume 8, No. 3, 2014

The Fifth Asia/Oceania Meteorological Satellite Users' Conference: GSICS Session

by Lawrence E. Flynn and Jaime Daniels, NOAA

The Fifth Asia/Oceania Meteorological Satellite Users' Conference (AOMSUC-5) was held November 19-21, 2014 in Shanghai, China. The conference was hosted by the China Meteorological Administration (CMA) and co-sponsored by World Meteorological Organization (WMO), Group on Earth Observations (GEO), Japan Meteorological Agency (JMA), Korea Meteorological Administration (KMA), and the Australian Bureau of Meteorology (BOM). There were approximately 150 attendees at the conference with representation from the world's satellite operators (CMA, KMA, JMA, EUMETSAT, Russian Federal Service for Hydrometeorology & Environmental Monitoring (ROSHYDROMET), and NOAA), WMO, research community, and the user community.

GSICS Session at the conference

The annual GSICS Users Workshop that was initially planned as part of the AOMSUC was included as a session in the conference and members gave a variety of presentations in this session. Peng Zhang, Chair of GSICS Executive Panel, gave a good overview of the GSICS activities in his keynote speech on the session. He described the GSICS products, their use and their maturity. Tim Hewison, Chair of GRWG introduced attendees to the upcoming products of GSICS. Larry Flynn Director GSICS Coordination Center gave a report about the new initiatives at the GSICS Coordination Center. Larry also presented a poster on Solar Backscatter measuring UV instruments on satellites in GEO and L1 positions, Likun Wang presented inter-comparison of AIRS, CrIS and IASI.

The GSICS session was informed of recent progress at CMA by a talk given by CMA scientist (Scott) Hu Xiuqing on new cross calibration products from CMA. Fuzhong Weng introduced the characterization of ATMS accuracy for GSICS products. Manik Bali provided a poster on retrieval of Spectral Response Function Using Hyper spectral Instruments.

Overall the GSICS session resulted in useful discussions.

AOMSUC Themes

In general, the AOMSUC also covered a broad set of themes that included:

a) Facilitation of data access and utilization and user preparation;

b) Application of satellite data to weather analysis, numerical weather prediction and nowcasting;

c) Application of satellite data to long term dataset for climate analysis, reanalysis and climate process studies;

d) Application of satellite data to environmental and disaster monitoring, disaster risk reduction

e) Atmospheric, land, and ocean parameters derived from satellite observations; and

The AOMSUC-5 program description, abstracts, and presentations can be found at this link: http://www.nsmc.cma.gov.cn/aomsuc5/.

The International Conference Steering Committee (ICSC), led by Dr. James Purdom, presented the statement for declaration of the Fifth Asia Oceania Meteorological Satellite User Conference and called for strong regional coordination in their satellite missions, data sharing and exchange of information in science, products and algorithms, and applications.

During the conference period, NESDIS Deputy AA Mark Paese and CMA/National Satellite Meteorological Center Director-in-general, Yang Jun also held one hour meeting and reviewed the progress of the NOAA-CMA bilateral activities related to satellite meteorology. Mark Paese also held a one hour meeting with Toshiyuki Kurino, Director of JMA's Meteorological Satellite Center (MSC) Data Processing Department, to discuss and review the progress of NOAA-JMA bilateral activities with a focus on activities related to Himawari-8.

Discuss the article

Return to Page 1

Announcements

Ralph Ferraro Accepts Chair of GSICS Microwave Subgroup

by Manik Bali

In the past year, the GSICS Microwave subgroup has been at the forefront of the activities of GSICS. It was lead by Cheng-Zhi Zou. Owing to change in roles at NOAA Cheng-Zhi Zou announced handing over the Microwave subgroup chair to Ralph Ferrao. Ralph Ferraro is the Chief of NOAA/NESDIS/STAR/Satellite Climate Studies Branch where he has held this position for the past ten years. He has worked the majority of his thirty year professional career conducting research on passive microwave sensor measurements and product applications.

His primary research interests are the retrieval of geophysical parameters from satellite-based passive microwave measurements and their applications at NOAA. This has included work with the Nimbus-7 SMMR, the DMSP SSM/I and SSMIS, the NOAA AMSU and MHS, the TRMM TMI , the Aqua AMSR, the GCOM AMSR-2, the S-NPP ATMS and the GPM GMI sensors. Several of the algorithms he has been developed are used operationally by FNMOC, NESDIS and NASA.

In addition to this, Ralph has been a focal point for an SSM/I time series that was a precursor to Climate Data Records (CDRs) - these data sets are still in production today at NCDC and have been extended to SSMIS.

Additionally, through a project supported by NCDC's CDR program, Ralph and his team have nearly completed an AMSU/MHS CDR data set that focuses on the window and water vapor channels.

Ralph hopes to exploit this expertise to develop some new initiatives for the GSICS MW-sub group that can lead to some new GSICS products for both sounders and imagers. He looks forward to working closely with current members of the subgroup and also expanding the membership.

2015 EUMETSAT Satellite conference to be held in Toulouse, France.

by Gabriele Kerrmann, EUMETSAT

The 2015 EUMETSAT Meteorological Satellite Conference will take place from 21 to 25 September 2015 in Toulouse, France. The First Announcement and Call for Papers is available on the EUMETSAT website at http://bit.ly/EMSC2015. Abstracts can be submitted from 1 December 2014 until 31 January 2015. You can submit your abstract on https://www.conftool.com/eumetsat2015/. We are planning to host the 2015 GSICS Users Workshop during one afternoon of this conference.

2015 NOAA Satellite conference to be held from April 27 – May 1, 2015 at Greenbelt, MD, USA

By Manik Bali, NOAA

NOAA is pleased to announce that the National Oceanic and Atmospheric Administration (NOAA) Satellite Conference for Direct Readout, GOES/POES, and GOES-R/JPSS Users, would be held from April 27 - May 1, 2015 in Greenbelt MD. The spotlight theme for this conference is "**Preparing for the future of the Environmental Satellites**"

One can Register at https://nsc2015.eventbrite.com/ Registration is a must for participants.

Submit your poster abstract at bit.ly/NSC2015posters through January 30, 2015.

Visit the conference website https://www.eventbrite.com/e/2015-noaa-satellite-conference-registration-12736973631 for more information.

Return to Page 1

GSICS-Related Publications

Chi, L., et al.,2014, Post Calibration of Channels 1 and 2 of Long-term AVHRR Data Record Based on SeaWiFS Data and Pseudo-invariant Targets. *Remote Sensing of Environment, 150*, 104-119

Doelling, D. R., et al., 2015, MTSAT-1R Visible Imager Point Spread Function Correction, Part I: The Need for, Validation of, and Calibration With. *IEEE Trans. Geosci. Remote Sens.*, Vol. 53, No. 3, 1513-1526, 10.1109/TGRS.2014.2344678

Du, J., et al., 2014, Inter-Calibration of Satellite Passive Microwave Land Observations from AMSR-E and AMSR2 Using Overlapping FY3B-MWRI Sensor Measurements. *Remote Sensing* Vol. 6 pp. 8594-8616

Efremova., et al., 2014, S-NPP VIIRS thermal emissive bands on-orbit calibration and performance, *Journal of Geophysical Research Atmos*., 119, 10,859–10,875, doi:10.1002/2014JD022078.

Khlopenkov, K., Doelling, D and Okuyama, A .,2015, MTSAT-1R Visible Imager Point Spread Function Correction, Part II: Theory. *IEEE Trans. Geosciences Remote Sens*., Vol. 53, No. 3, 1504-1512, 10.1109/TGRS.2014.2344627

Ma,S., Yan, W., Huang, Y., Ai, W and Zhao, X ., 2015, Vicarious calibration of S-NPP/VIIRS day night band using Deep Convective Clouds. *Remote Sensing of Environment*, 158, 42–55, doi:10.1016/j.rse.2014.11.006

Maidment, R. I., Grimes, D., Allan, R, P., Tarnavsky, E., Stringer, M., Hewison, T., Roebeling and Black, E .,2014, The 30 year TAMSAT African Rainfall Climatology And Time series (TARCAT) data set. *Journal of Geophysical Research Atmos*, 119, 10,619–10,644 doi:10.1002/2014JD021927.

Quan, W.,2014, Vicarious Cross-Calibration of the China Environment Satellite Using Nearly Simultaneously Observations of Landsat-7 ETM+ Sensor. *Journal of Indian Society of Remote Sensing*, Vol. 42 No. 3 pp. 539-548

Yu, F., Wu, X., Grotenhuis, M and Qian, H .,2014, Inter-calibration of GOES Imager visible channels over the Sonoran Desert. *Journal of Geophysical Research Atmos*., 119, 8639–8658, doi:10.1002/2013JD020702.

Zou, X., Weng, F and Yang, H.,2014, Connecting the Time Series of Microwave Sounding Observations from AMSU to ATMS for Long-Term Monitoring of Climate. *J. Atmos. Oceanic Technol.*, 31, 2206–2222.
doi: http://dx.doi.org/10.1175/JTECH-D-13-00232.1

Submitting Articles to GSICS Quarterly Newsletter:

The GSICS Quarterly Press Crew is looking for short articles (~700 words with one or two key, simple illustrations), especially related to cal/val capabilities and how they have been used to positively impact weather and climate products.
Unsolicited articles are received for consideration anytime, and if accepted, will be published in the next available newsletter issue after approval/editing. Note the upcoming spring issue will be a general issue. Please send articles to manik.bali@noaa.gov.

With Help from our Friends:

The GSICS Quarterly Editor would like to thank David R. Doelling, Chair of GSICS VIS Subgroup for the lead article in this issue and for reviewing all of the other articles in this special issue on VIS Calibration. Dave was supported by members of the GSICS Quarterly Editorial Board.

Editorial Board
Manik Bali , Editor
Lawrence E. Flynn, Reviewer
Lori K. Brown, Proof reader and Tech Support
FangFang Yu, American Correspondent.
Tim Hewison, European Correspondent
Yuan Li, Asian Correspondent

Special thanks to Bob Kuligowski

The editor would also like to thank Bob Kuligowski for proofreading the newsletter articles. Bob recently received the 2015 Bulletin of the AMS Editor's Award, and his participation in the review process has helped us to maintain the high standards of the newsletter.

Return to Page 1